Identification of low-lying proton-based intruder states in $^{189-193}$Pb

K. Van de Vel
Instituut voor Kern–en Stralingsfysica, University of Leuven, Celestijnenlaan 200 D, 3001 Leuven, Belgium

A. N. Andreyev,* M. Huyse, and P. Van Duppen
Instituut voor Kern–en Stralingsfysica, University of Leuven, Celestijnenlaan 200 D, 3001 Leuven, Belgium

J. F. C. Cocks,† O. Dorvaux,‡ P. T. Greenlees, K. Helariutta,§ P. Jones, R. Julin, S. Juutinen, H. Kettunen, P. Kuusiniemi, M. Leino, M. Muikku,‖ and P. Nieminen
Department of Physics, University of Jyväskylä, 40351 Jyväskylä, Finland

K. Eskola
Department of Physics, University of Helsinki, Helsinki, Finland

R. Wyss
Department of Physics, Royal Institute of Technology, 104 05 Stockholm, Sweden
(Received 4 March 2002; published 22 May 2002)

Low-lying proton-based intruder states have been observed in the odd-mass isotopes ^{189,191,193}Pb in experiments at the RITU gas-filled recoil separator. The identification has been performed by observing the fine structure in the α decay of the parent ^{193,195,197}Po nuclei in prompt coincidence with conversion electrons and γ rays in the daughter lead isotopes. Along with the literature data these results establish a systematics of intruder states in the odd-mass lead isotopes from ^{197}Pb down to ^{185}Pb. Interpretation of these states involves the coupling of the $1i_{13/2}$ or $3p_{3/2}$ odd neutron to the 0^+ state in the oblate minimum in the even-mass lead core. Conversion coefficients have been determined for some of the transitions, revealing mixing between the coexisting states. The experimental results are compared to potential energy surface calculations.

DOI: 10.1103/PhysRevC.65.064301 PACS number(s): 23.60.+e, 21.10.Tg, 21.60.Cs, 27.80.+w

I. INTRODUCTION

Within the last decade the neutron-deficient lead isotopes became the subject of extensive experimental and theoretical studies, and a wealth of information on shape coexistence in these nuclei was obtained; see [1–4] for a review. As a result of the shell closure at $Z=82$, lead nuclei are spherical in their ground state (g.s.), but at higher excitation energies a subtle interplay between configurations with different shapes—oblate and prolate—has been predicted [5,6]. This has been observed experimentally; see, for example, recent in-beam and decay studies of the even-mass nuclei $^{182-192}$Pb ([4,7–19] and references therein).

In particular, low-lying 0^+ π [two-particle–two-hole $(2p\text{-}2h)$] proton-based intruder bandhead states (i.s.), associated with a deformed oblate shape, have been identified via β- and α-decay studies in the even-mass lead nuclei down to ^{190}Pb (see, for instance, [12,20]) and recently in ^{188}Pb [13–15] and in ^{186}Pb [17]. The excitation energy of these states shows a nearly parabolic dependence on the valence neutron number with a predicted minimum [6] close to the neutron midshell at $N=104$; the intruder states even become the first excited states in $^{186-194}$Pb. In some cases a rotationlike band built on top of the intruder state has been identified. Consistent with theoretical predictions [2,6], prolate rotational bands, presumably of $\pi(4p\text{-}4h)$ or $\pi(6p\text{-}6h)$ character, have been observed in ^{182,184,186,188}Pb. In alpha-decay studies the corresponding prolate 0^+ bandhead can be populated, as, for example, in ^{186}Pb [17]. In agreement with theoretical predictions, the energy separation between the coexisting oblate and prolate 0^+ states in ^{186}Pb was found to be rather small, of the order of 150 keV.

In the odd-mass lead nuclei the coupling of a valence neutron to the states in the spherical, oblate, and prolate minima in the neighboring even-mass lead core is expected to result in corresponding coexisting configurations. Rather extensive systematics of excited states exist for the odd-mass lead nuclei with $A \geqslant 193$ [21]; recent in-beam studies of the light odd-mass lead isotopes identified the lowest positive-parity states in ^{187,189,191}Pb [22–24]. The structure of the low-lying states in $^{187-199}$Pb can be interpreted as a weak coupling of the odd $1i_{13/2}$ neutron to the low-lying spherical states of the even lead core. In ^{191,193,195,197}Pb dipole bands have been observed which were interpreted as $M1$ cascades, resulting from the coupling of the $1i_{13/2}$ neutron hole to two

*Present address: Department of Physics, Oliver Lodge Laboratory, University of Liverpool, P.O. Box 147, Liverpool L69 7ZE, UK.

†Present address: BNFL Seascale Cumbria, CA20 1PG, UK.

‡Present address: Institut de Recherches Subatomiques, F-67037 Strasbourg cedex 2, France.

§Present address: Laboratory of Radiochemistry, Department of Chemistry, University of Helsinki, P.O. Box 55, Helsinki, Finland.

‖Present address: Steilyturvakeskus Laippatie, Helsinki, Finland.

protons excited across the $Z=82$ shell gap, occupying the $1h_{9/2}$ and $1i_{13/2}$ intruder orbitals at small oblate deformation (see, for example, [21,24] and references therein). However, in contrast to the even-mass lead nuclei, information on the low-lying deformed intruder bandheads is scarce. Excited $13/2^+$ states have been observed in the high-spin isomer in ^{195,197}Pb (via β-decay studies of the parent Bi nuclei [25,26]) and in ^{187}Pb (via the α decay of ^{191}Po [27,28]). These states are interpreted as the coupling of the $1i_{13/2}$ valence neutron to the oblate $\pi(2p\text{-}2h)$ 0^+ bandheads in the even-mass lead core. Furthermore, in a recent fine-structure α-decay study of ^{189}Po [18], a low-lying excited state has been found in ^{185}Pb which could be tentatively interpreted as the first observation of a prolate deformed intruder state in the odd-mass lead nuclei.

In the low-spin isomer in ^{187}Pb an oblate intruder state, resulting from the coupling of a $3p_{3/2}$ neutron to the oblate 0^+ state in the even-even core, has been observed [27,28].

In this paper we report on the observation, through fine structure in the α decay of ^{193,195,197}Po, of low-lying proton-based intruder states in the daughter ^{189,191,193}Pb isotopes. Preliminary data from this study were given in [29]. Section II of the paper gives the details on the experimental setup and in Sec. III we present the experimental data, which are further discussed in Sec. IV on the basis of potential energy surface (PES) calculations. Conclusions are given in Sec. V.

II. EXPERIMENTAL SETUP

The experiment was performed at the gas-filled recoil separator RITU [30] at the Accelerator Laboratory of the University of Jyväskylä (JYFL). The ^{193}Po nuclei were produced in the ^{166}Er(^{32}S,5n)^{193}Po [$E_{lab}(^{32}\mathrm{S})=169$ MeV] reaction, while the ^{195}Po nuclei were studied in the ^{169}Tm(^{32}S,$p5n$)^{195}Po [$E_{lab}(^{32}\mathrm{S})=188$ MeV] and ^{160}Dy(^{40}Ar,5n)^{195}Po [$E_{lab}(^{40}\mathrm{Ar})=189$ MeV] reactions. The nucleus ^{197}Po was produced in the latter reaction on the admixtures of the heavier dysprosium isotopes in the target. Self-supporting targets of ≈ 500 μg/cm^2 thickness were exploited with an enrichment of 96%, 100%, and 67% for ^{166}Er, ^{169}Tm, and ^{160}Dy, respectively. Pulsed beams (2 ms on /8 ms off) of ^{32}S and ^{40}Ar, delivered by the $K=130$ cyclotron, were used with an average intensity of about 15 pnA after pulsing.

The recoiling fusion-evaporation products, after passing through the separator, were implanted into a 35 mm $\times$80 mm, 300-μm-thick position-sensitive silicon strip detector (PSSD), where their subsequent α-particle decays were registered. The energy resolution of the individual strips was about 20 keV. Four germanium detectors were installed a few cm behind the PSSD for the measurement of prompt and delayed (up to a few μs) α-γ-ray and α-x-ray coincidences. The energy calibration and absolute efficiency determination of the germanium detectors were performed using an intensity-calibrated ^{60}Co source and mixed ^{152}Eu/^{133}Ba γ-ray sources. At the backward hemisphere the PSSD was surrounded by six 5 cm$\times$5 cm, 456-μm-thick silicon detectors [further referred to as electron detectors (EDs)], forming a 5 cm$\times$10 cm, 5-cm-deep box, open from two opposite sides to let the recoils pass through. These detectors were used to detect conversion electrons (CEs) escaping from the PSSD in prompt coincidence with the fine structure α decays of the parent polonium nuclei feeding low-lying excited states in the daughter lead isotopes. Also α and β particles escaping from the PSSD without depositing their full energy were detected in the electron detectors. The low-energy ($E_{e^-}\leqslant 800$ keV) part of the spectra in the EDs was roughly calibrated with an ^{133}Ba source. The determination of the absolute efficiency of the EDs necessary for the calculations of conversion coefficients will be discussed further in the text. More details on the application of this method are given elsewhere [14,18]. In the data analysis, α-particle decays in the PSSD were searched for in prompt coincidence with either low-energy signals in the EDs or with γ-ray events in the germanium detectors.

III. EXPERIMENTAL RESULTS

A. Excited states of ^{189m,g}Pb

To illustrate the analysis procedure, we present a detailed discussion of the ^{193m,g}Po$\rightarrow^{189m,g}$Pb decay. Figure 1(a) shows a singles α-particle spectrum, collected between beam pulses for the ^{32}S+^{166}Er reaction. In addition to ^{193g}Po [$E_\alpha=6949(5)$ keV] and ^{193m}Po [$E_\alpha=7004(5)$ keV] [31], other α-particle emitters—for example, ^{194}Po and ^{193}Bi—were produced with higher cross sections. Figure 1(b) shows the same α-particle spectrum but requiring a prompt ($\Delta T_{\alpha\text{-}e^-}<40$ ns) coincidence with a low-energy signal ($E_{e^-}\leqslant 700$ keV) from the backward EDs. Two α lines at $E_\alpha=6194(20)$ keV and $E_\alpha=6375(15)$ keV are clearly observed in Fig. 1(b).

The first line at 6194 keV is associated with the known fine-structure α decay of ^{194}Po [$E_\alpha=6194(7)$ keV, $b_\alpha=0.22\%$] to an excited 0^+ $\pi(2p\text{-}2h)$ intruder state at 658 keV in ^{190}Pb, decaying further solely by conversion electron emission to the 0^+ g.s. [32]. By comparing the intensity of this line (after normalization to the known branching ratio b_α) with the intensity of the g.s$\rightarrow$g.s. ($E_\alpha=6842$ keV) α decay of ^{194}Po [Fig. 1(a)], the absolute efficiency of the EDs for 570 keV conversion electrons was deduced. As the deduced efficiency value applies to electrons with an energy of $E_{e^-}=658$ keV$-B_{e^-}$, where B_{e^-} is the electron binding energy in the daughter lead nucleus, the electron efficiency for other energies was deduced using GEANT Monte Carlo calculations [33], normalized to the above experimental value.

The α line at 6375 keV was assigned to the α decay of ^{193m}Po to an excited state at 637(1) keV in the daughter ^{189m}Pb nucleus. This assignment is based on the observation of nine 6375(15)–637(1) keV α-γ coincident pairs in the prompt ($\Delta T_{\alpha\text{-}\gamma}\leqslant 40$ ns) α-γ matrix; see Fig. 1(c). The sum Q value $Q_{\alpha,sum}=7147$ keV for the 6375–637 keV α-γ pairs is similar to the $Q_\alpha=7152$ keV value of the $E_\alpha=7004$ keV g.s.$\rightarrow$g.s. α decay of ^{193m}Po. There is a small shift to higher energies of the α-particle energies of 10–15

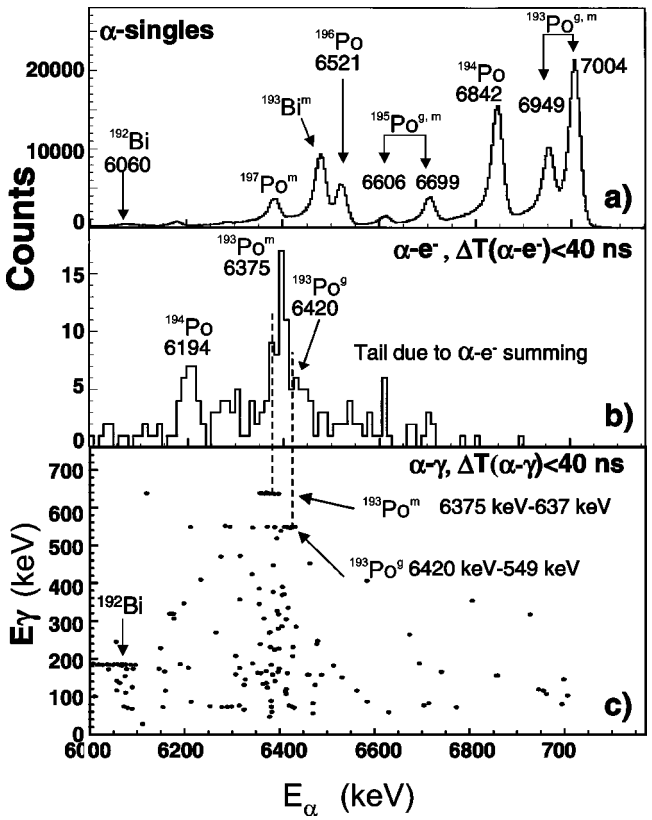

FIG. 1. (a) Singles α-particle energy spectrum measured in the $^{32}S+^{166}Er$ reaction in between beam pulses. (b) The same spectrum as in (a) but a prompt coincidence with a low-energy signal in the EDs is required. (c) Prompt ($\Delta T_{\alpha\text{-}\gamma} \leqslant 40$ ns) α-γ coincidence matrix for the events from spectrum (a). Arrows point to α-γ coincidence events that are labeled with the α-particle and γ-ray energies (in keV) and the isotope the α decay belongs to. The α-particle energy labels in (b) are corrected for α-CE summing; see discussion in the text.

keV in the α-e^- spectrum [Fig. 1(b)] compared to values deduced from the α-γ spectrum [Fig. 1(c)]. This shift is due to summing in the PSSD of the α-particle energy with the energy, left by the conversion electron in the PSSD while escaping to the backward detectors, as discussed in [14,18]. This energy loss is in agreement with calculations performed with the GEANT Monte Carlo code [33], taking into account the experimentally measured (X,Y, depth, intensity) position-implantation depth-intensity distribution of the recoils in the PSSD. The energy labels of the peaks in Fig. 1(b) were corrected for this effect.

Similarly, fine structure in the α decay of ^{193g}Po populating an excited level at 549 keV in the daughter ^{189g}Pb was identified by observing eight 6420(20)–549(1) keV α-γ coincident pairs [Fig. 1(c)] with the corresponding value of $Q_{\alpha,sum}=7104$ keV, close to the value of $Q_\alpha=7096$ keV for the 6949 keV α decay of ^{193g}Po. In the α-e^- coincidence spectrum [Fig. 1(b)] a corresponding weak α transition at $E_\alpha=6420(20)$ keV could be tentatively observed as a shoulder of the more abundant peak at $E_\alpha=6375$ keV.

The prompt character of the observed α-γ coincidences limits the multipolarity of the 637-keV and 549-keV γ-ray transitions to $L\leqslant 2$. Furthermore, by comparing the numbers of α-γ and α-e^- events for the $E_\alpha=6375$ keV α decay, after correcting for the corresponding γ-ray and electron efficiency, a total conversion coefficient of $\alpha_{tot}=1.1(4)$ for the 637 keV transition was deduced. The deduced conversion coefficient value is larger than the theoretical values [34] for $L\leqslant 2$ transitions [$\alpha_{tot}(E2)=0.017$, $\alpha_{tot}(M1)=0.06$, and $\alpha_{tot}(M2)=0.16$], indicating a strong $E0$ component in the 637 keV transition. Similarly, a total conversion coefficient $\alpha_{tot}=0.34(16)$ for the 549 keV transition was deduced, to be compared with the theoretical values of $\alpha_{tot}(E2)=0.024$, $\alpha_{tot}(M1)=0.088$, or $\alpha_{tot}(M2)=0.25$. The latter value is consistent, within the error bars, with the measured value. However, as we will show further, a parity-changing $M2$ assignment can be ruled out. Therefore the 549 keV transition should be of mixed $E0$-$M1$-$E2$ character.

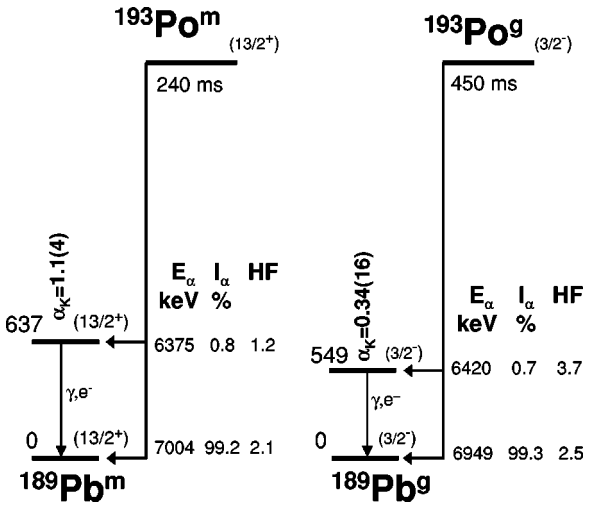

FIG. 2. Alpha-decay scheme of ^{193m,g}Po. Indicated are α-particle energies, intensities, and hindrance factor values (see Sec. III). Spin and parity assignments are discussed further in the text.

The given uncertainties of the conversion coefficients are mainly determined by the number of α-γ and/or α-e^- events registered and by the uncertainty of about $\approx$20% in the EDs efficiency determination.

By comparing the number of registered 7004 keV and 6949 keV α decays between beam pulses and the corresponding sum of α-e^- and α-γ events (corrected for e^- and γ-ray detection efficiencies), branching ratio values of $b_\alpha=0.8(3)\%$ for $E_\alpha=6375$ keV and $b_\alpha=0.7(3)\%$ for $E_\alpha=6420$ keV α decays were derived. Based on these data, hindrance factor (HF) values were deduced which provide crucial information on the spin, parity, and configurations of the states connected by the α decay. The α-decay scheme of ^{193m,g}Po is shown in Fig. 2; decay data are given in Table I. The discussion on the configurations and I^π assignments will be given in Sec. IV.

B. Excited states of ^{191m,g}Pb and ^{193m}Pb

Similarly to the case of ^{193m,g}Po, fine structure in the α decay of ^{195m,g}Po and of ^{197m}Po has been identified on the

TABLE I. The α-particle energies (E_α), intensities (I_α), and HF values for the "main" and fine-structure (f.s.) α decays of the $I^\pi = 13/2^+$ and $I^\pi = 3/2^-$ states in Po nuclei along with the spin and parity (I^π) and excitation energies (E^*) (relative to the lowest-energy state of the same spin and parity) of the excited states in the Pb nuclei. The total conversion coefficients (α_{expt}) and multipolarity for some transitions are given in the last two columns, respectively.

	^{A}Po				$^{A-4}$Pb			
	E_α (keV)	I_α (%)	HF	I^π (Po)	I^π (Pb)	E^* (keV)	α_{expt}	Mult.
^{193g}Po$\rightarrow$ ^{189g}Pb	6949(10)	99.3(25)	2.5(3)	$3/2^-$	$3/2^-$	0		
f.s.	6420(20)	0.7(3)	3.7(16)	$3/2^-$	$3/2^-$	549(1)	0.34(16)	$E0$-$M1$-$E2$
^{193m}Po$\rightarrow$ ^{189m}Pb	7004(10)	99.2(35)	2.1(3)	$13/2^+$	$13/2^+$	0		
f.s.	6375(15)	0.8(3)	1.2(4)	$13/2^+$	$13/2^+$	637(1)	1.1(4)	$E0$-$M1$-$E2$
^{195g}Po$\rightarrow$ ^{191g}Pb	6606(10)	99.8(35)	2.43(14)	$3/2^-$	$3/2^-$	0		
f.s.	6030(20)	$\geqslant$0.17(5)	$\leqslant$6.5(19)	$3/2^-$	$3/2^-$	597(1)		
^{195m}Po$\rightarrow$ ^{191m}Pb	6699(10)	99.8(25)	1.96(18)	$13/2^+$	$13/2^+$	0		
f.s.	6050(20)	0.20(12)	2.8(15)	$13/2^+$	$13/2^+$	670(1)	0.8(3)	$E0$-$M1$-$E2$
^{197m}Po$\rightarrow$ ^{193m}Pb	6385(10)	99.3(35)	2.0(2)	$13/2^+$	$13/2^+$	0		
f.s.	5622(25)	$\geqslant$0.05(3)	$\leqslant$1.7(10)	$13/2^+$	$13/2^+$	757(1)		

basis of the Q_α sum-energy balance, by analyzing prompt α-γ and α-electron coincidences collected for the corresponding reactions.

For ^{195m}Po and ^{195g}Po coincident pairs of 6050(20)–670(1) keV α-γ (nine events) and 6030(20)–597(1) keV α-γ (six events) were observed, respectively. This establishes excited states at 670(1) keV in ^{191m}Pb and at 597(1) keV in ^{191g}Pb. In addition, an α line at $E_\alpha = 6065(20)$ keV [$N_{\alpha\text{-}e^-} = 43(6)$ α-e^- events] in the α-particle spectrum gated by the electrons in the EDs was observed. After correcting for an energy shift of 10–15 keV due to α-e^- summing (see above), an "unshifted" α-particle energy of $E_\alpha = 6050(25)$ keV was deduced, which fits well to the 6050(20)-keV fine-structure α decay of ^{195m}Po and is too high to be consistent with the 6030(20)-keV fine-structure α decay of ^{195g}Po. On this ground the conversion electrons coincident with the fine-structure α decay of 6050(25) keV were attributed as resulting from the deexcitation of the 670 keV level in ^{191m}Pb and a conversion coefficient of $\alpha_{tot} = 0.8(3)$ for the 670 keV transition could be deduced. A comparison of the measured and theoretical [$\alpha_{tot}(M2) = 0.14$, $\alpha_{tot}(M1) = 0.053$, and $\alpha_{tot}(E2) = 0.015$] conversion coefficients shows also here the presence of a strong $E0$ component in the 670 keV transition in ^{191m}Pb.

For ^{197m}Po two α-γ coincident pairs with 5622(25)–757(1) keV have been found, which result in a sum $Q_{\alpha,sum}$ value of 6496(25) keV. This value is in agreement (within 1σ) with the value of $Q_\alpha = 6517$ keV for the 6385 keV g.s.$\rightarrow$g.s. α decay of ^{197m}Po. Therefore we tentatively identify an excited state at 757(1) keV in ^{193m}Pb. Anticipating the discussion in Sec. IV, we mention that the excitation energy of this state fits well in the systematics of the $13/2^+$ intruder states in the odd-mass lead nuclei with $189 \leqslant A \leqslant 197$.

As a result of low statistics and a rather high background in the α-e^- coincidence spectra, we were not able to extract the number of α-e^- coincidences for ^{195g,197m}Po; consequently, no conversion coefficients for the 597 keV and 757 keV transitions could be deduced.

The experimental results for the α decay of ^{193,195,197}Po are summarized in Table I. The hindrance factors, spin and parity assignments, and multipolarity values for some γ-ray transitions are discussed in Sec. IV. We mention that in the case of the α decay of ^{195g,197m}Po the deduced branching ratios and hindrance factor values represent lower and upper, respectively, limits because of the nonobservation of α-e^- coincidences.

IV. DISCUSSION

As discussed in our previous work [12,27], α-decay fine-structure measurements are a powerful tool to identify and to study low-lying intruder states. The α-decay hindrance factors can provide information on the structure of the states involved in both parent and daughter nuclei. In the daughter nucleus the characteristics of the decay of the intruder states gives information concerning the mixing between the coexisting states. Additional information on the structure of the different states involved in the α decay is provided by PES calculations.

A. Spin and parity assignment to the excited states identified in ^{189,191,193}Pb

Unfortunately, no direct I^π measurements have been reported for the ground state and isomeric state of polonium isotopes with $A \leqslant 197$ and for lead isotopes with $A \leqslant 193$ [21]. However, based on well-established systematics for heavier odd-mass polonium and lead isotopes, the $I^\pi = 13/2^+$ assignment to the α-decaying states of ^{193m,195m,197m}Po and to the respective daughter products ^{189m,191m,193m}Pb as well as the $3/2^-$ spin and parity assignments to ^{193g,195g}Po and ^{189g,191g}Pb have been suggested by many authors [21]. According to systematics and available experimental data these states are explained by a weak coupling of the $1i_{13/2}$ or $3p_{3/2}$ valence neutron to the 0^+ spherical states in the even-mass neighbors (see, for example, [22,24,36] and references therein). The assignment of

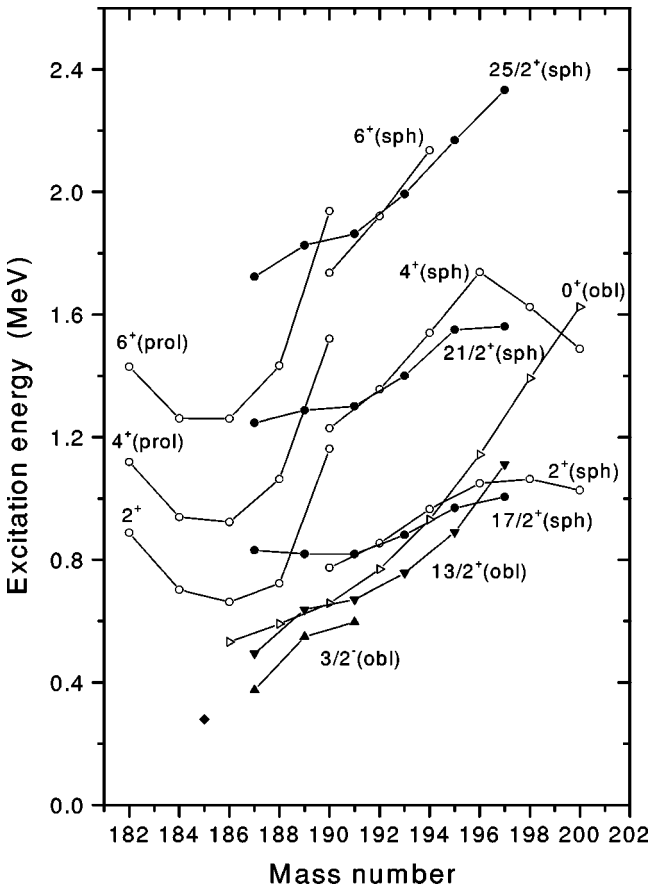

FIG. 3. Low-energy level systematics for selected configurations in the light lead isotopes. Yrast states are indicated by circles, 0_2^+ states by empty right triangles, $13/2_2^+$ states by filled down triangles, and $3/2_2^-$ states by filled up triangles. The data for ^{185}Pb from [18] are shown with a solid diamond. Suggested deformation assignments to most of the states are indicated. The excitation energies are shown relative to the 0^+ ground state in the even-mass nuclei, and relative to the lowest $3/2^-$, $13/2^+$ states, for the negative- and positive-parity states, respectively, in the odd-mass nuclei. Results are taken from [7–10,13,15,17–26] and the present work.

the same spin and parity to the parent and daughter nuclei within each decay chain is strongly supported by the low hindrance factor values HF$\approx$(2–2.5) for the α transitions between the respective states (Table I). The HF of odd-mass nuclei is defined as the ratio of the reduced α width δ_α^2, calculated by the method of Rasmussen [37], of the transition relative to the reduced α width of the unhindered g.s. $\rightarrow$g.s. ($\Delta L=0$) transitions in the even-even neighbors. An HF value less than 4 implies unhindered decay between states of equal spin, parity, and configuration [35]. The slight retardation of the α decay of the odd Po isotopes, compared to the $0^+\rightarrow 0^+$ transitions in the neighboring even-even cores, can be qualitatively understood as a result of a blocking effect by the $3p_{3/2}$ or $1i_{13/2}$ odd neutron. Assuming that the α particle is essentially formed at the nuclear surface, the occupation of an orbital at the Fermi surface by an odd particle will reduce the α-particle formation probability, analogous to the well-known reduction in pairing correlations. As a result of a different number of sub-orbitals (2 and 7, respectively), the blocking of a single suborbital in the $3p_{3/2}$ orbital appears to have higher impact on the α-particle formation probability (reduced width δ_α^2) compared to the blocking of a single suborbital in the $1i_{13/2}$ orbital. This is indeed seen from the present data, as the α decay between the $3/2^-$ states of Po and Pb (^{191g,193g,195g}Po) has a systematically slightly higher hindrance factor (HF$\approx$2.5), compared to the decay between the $13/2^+$ states (HF$\approx$2 in ^{193m,195m,197m}Po); see Table I.

We emphasize the importance of underlying configurations when evaluating hindrance factors. In the ^{191}Po $\rightarrow^{187}$Pb case, as discussed in Refs. [27,28], the 7378 keV α decay proceeds between two $13/2^+$ states. This decay is strongly hindered (HF=26) due to different configurations involved [pure intruder $\nu(1i_{13/2})\otimes\pi(4p\text{-}2h)$ in ^{191}Po and normal $\nu(1i_{13/2})\otimes\pi(0p\text{-}0h)$ in ^{187}Pb]. This strong hindrance is also evident from the long half-life $T_{1/2}$ =93(3) ms of the $13/2^+$ state, to be compared to the $3/2^-$ state in ^{191}Po with nearly the same α energy of 7334 keV, but a half-life of 22 ms; see discussion in [27].

We can further use the HF values to deduce information on the spin and parity of the excited states in ^{189,191,193}Pb, identified in our work. The low HF values for the fine-structure α decays of ^{193,195,197}Po establish the same spin and parity for the states connected by these decays: $I^\pi=13/2^+$ have been assigned to the excited states, identified in ^{189m,191m,193m}Pb and $I^\pi=3/2^-$ to the excited states in ^{189g,191g}Pb; see Table I. We remind the reader that some of the hindrance factor values in Table I (including HF$\leqslant$6.5 for ^{191g}Pb) are upper limits only (see Sec. III B). Furthermore, in some cases (^{189,191m}Pb) the spin and parity assignment to the excited states is supported by a strong $E0$ component in the decay of these excited states. The prompt character of the α-γ coincidences together with the low HF values excludes a parity-changing $M2$ component in the decay of the excited states, resulting in a mixed $E0$-$M1$-$E2$ character of the transitions.

B. Oblate intruder states

The low-energy level systematics of the lead nuclei with $182\leqslant A\leqslant 200$ relevant for further discussion is shown in Fig. 3. As the energy difference between the isomeric $13/2^+$ and $3/2^-$ states is not known for the odd-mass Pb nuclei, the excitation energy of the negative- and positive-parity states is given relative to the lowest $3/2^-$ and $13/2^+$ states, respectively. The values are taken from [7–10,13,15,17–26] and the present work.

In the odd-mass isotopes with $A\geqslant 191$ the $17/2^+$, $21/2^+$, and $25/2^+$ states closely follow the 2^+, 4^+, and 6^+ levels of the yrast band in the neighboring even-mass nuclei. As mentioned above, this pattern can be explained by the weak coupling of the odd $1i_{13/2}$ neutron to the ground state band in the neighboring even-even core; see [22,24] and references therein. The ground state band in these cases is of spherical character although some mixing with the intruding oblate states occurs [38].

For nuclei with $A<190$ the observed band structure in the odd- and even-mass lead isotopes differs considerably. The yrast states with $I^{\pi}\geqslant 4^{+}$ in the even-mass $^{182-188}$Pb isotopes show an abrupt change compared to the yrast band of the heavier Pb isotopes. The nearly parabolic behavior of these yrast states with a minimum around $N=103$ can be associated with a prolate $\pi(4p\text{-}4h)$ structure intruding to low energy [6–9,19]. In contrast, the yrast states in ^{187,189}Pb do not drop down in energy as much as in the even-mass nuclei. The $17/2^{+}$, $21/2^{+}$, and $25/2^{+}$ states are believed [22] to result from the weak coupling of the odd $1i_{13/2}$ neutron to the (yet unobserved) spherical states in the even-even core, which presumably become nonyrast in the light even-mass lead nuclei, although admixtures from a prolate structure, resulting from the strong coupling of the odd neutron to the even-even core, cannot be ruled out [22].

The excitation energy of the oblate 0^{+} $\pi(2p\text{-}2h)$ intruder bandheads in the even-mass lead nuclei with $A\geqslant 186$ also shows a parabolic dependence as a function of the neutron number [12–17]. These states become the first excited states in $^{186-194}$Pb and the hindrance factor for the fine-structure α decay to these states evolves from 2.8 in ^{194}Pb to 0.56 in ^{186}Pb [12–14,17].

Figure 3 clearly demonstrates that the behavior of the $13/2^{+}$ excited states in $^{189m-193m}$Pb, identified in this work, along with the literature data on ^{195m,197m}Pb [25,26], follows closely the behavior of the 0^{+} oblate intruder states in the even-mass lead core and the same trend is observed for the $3/2^{-}$ excited states in ^{189g,191g}Pb. Furthermore, similar to the 0^{+} oblate intruder states in $^{188-194}$Pb, the $13/2^{+}$ and $3/2^{-}$ excited states become the first excited states in the $^{189-191}$Pb nuclei.

Therefore the observed low-lying states in the odd Pb isotopes are interpreted as intruder states, resulting from the coupling of an odd $1i_{13/2}$ neutron ($^{189m-197m}$Pb) or $3p_{3/2}$ neutron (^{189g,191g}Pb) to the 0^{+} band head of the oblate $\pi(2p\text{-}2h)$ configuration in the even-even lead core.

As discussed in Refs. [4,32], the ground state wave function of light Po nuclei contains both a nearly spherical normal and deformed intruder component. By comparing the transition strength of the α decay of Po to the oblate intruder state and spherical state of the daughter Pb nuclei, one can obtain information on the configurations present in the ground state of Po. The reduced α width values δ_{α}^{2} are plotted as open symbols as a function of neutron number for the g.s.$\rightarrow$g.s. ($0^{+}\rightarrow 0_{1}^{+}$) decay of the even-mass Po and Rn nuclei [Fig. 4(a)] and for the $13/2^{+}\rightarrow 13/2_{1}^{+}$ and $3/2^{-}\rightarrow 3/2_{1}^{-}$ decays of odd-mass Po [Fig. 4(b)]. Data are taken from [12,13,15,17,18,21,27,28,32,39]. We note that the data for ^{188,189}Po are preliminary; based on intensities from [18], no I^{π} assignment to ^{189}Po has been made so far. Unlike heavier nuclei [see, for example, the even-mass Rn isotopes in Fig. 4(a), where a gradual increase in the reduced width is observed when moving away from the $N=126$ closed shell], the δ_{α}^{2} values for the even- and odd-mass Po nuclei remain constant down to $N=106$. Wauters *et al.* [32] showed that the saturation behavior for even-mass Po nuclei is due to the increasing $\pi(4p\text{-}2h)$ intruder admixture in the ground state

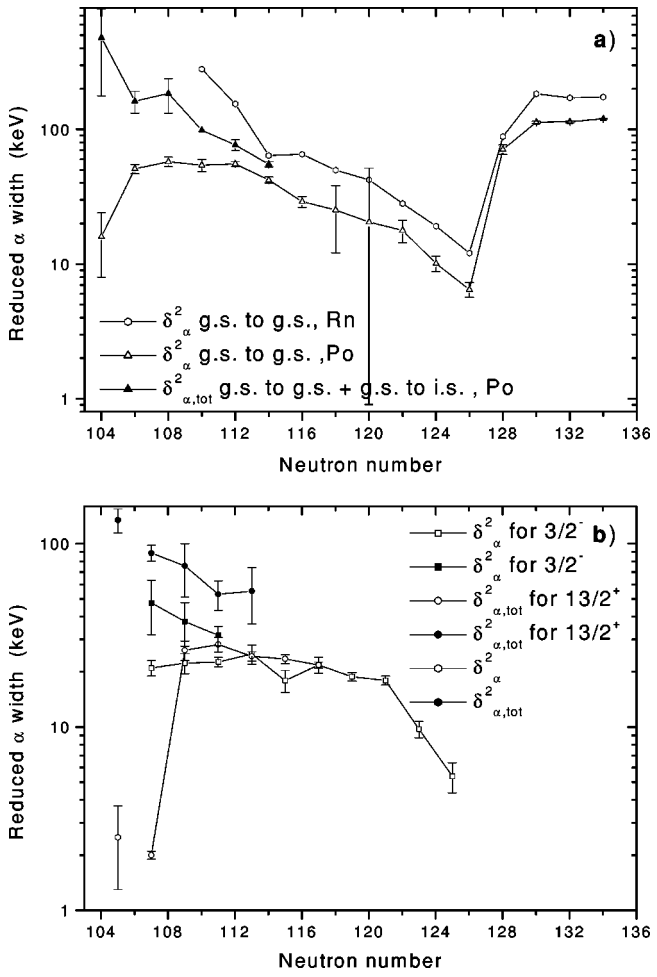

FIG. 4. (a) Reduced α widths as a function of neutron number for the $0^{+}\rightarrow 0_{1}^{+}$ decay, δ_{α}^{2}, of Po (open triangles) and Rn (open diamonds), and for the sum of the $0^{+}\rightarrow 0_{1}^{+}$ and $0^{+}\rightarrow 0_{2}^{+}$ decay of Po, $\delta_{\alpha,tot}^{2}$ (solid triangles). (b) The same as in (a) but for the decay of the $13/2^{+}$ (circles) and $3/2^{-}$ (squares) states in the odd-mass Po isotopes to the $13/2^{+}$, $3/2^{-}$, respectively, states in Pb. Data are taken from [12,13,15,17,18,21,27,28,32,39].

of the Po mother nucleus. The decay to the spherical $\pi(0p\text{-}0h)$ 0_{1}^{+} ground state of Pb is retarded, while the α decay to the excited $\pi(2p\text{-}2h)$ 0_{2}^{+} intruder states in Pb is getting increasingly favored when moving towards the neutron midshell. Indeed, by summing up the reduced widths for the α decay to the ground and excited 0^{+} states ($\delta_{\alpha,tot}^{2}$, shown by solid symbols), where data for the fine-structure decay are known, the expected increase in δ_{α}^{2} when moving away from the $N=126$ closed neutron shell is reproduced. From Fig. 4(b) it is clear that the total reduced width ($\delta_{\alpha,tot}^{2}$) of the α decay of the odd Po isotopes behaves in a similar way. The sudden drop in the δ_{α}^{2} values of ^{189,191m}Po is possibly due to a structure change, as discussed in Refs. [18,27,28]. From the Po reduced-α-width plot it is also clear that the α decay of the odd-mass Po nuclei is slower compared to the even-mass nuclei; furthermore, the decay of the $3/2^{-}$ state is more hindered compared to the $13/2^{+}$ state. Both facts are qualitatively explained by a blocking effect, as discussed above.

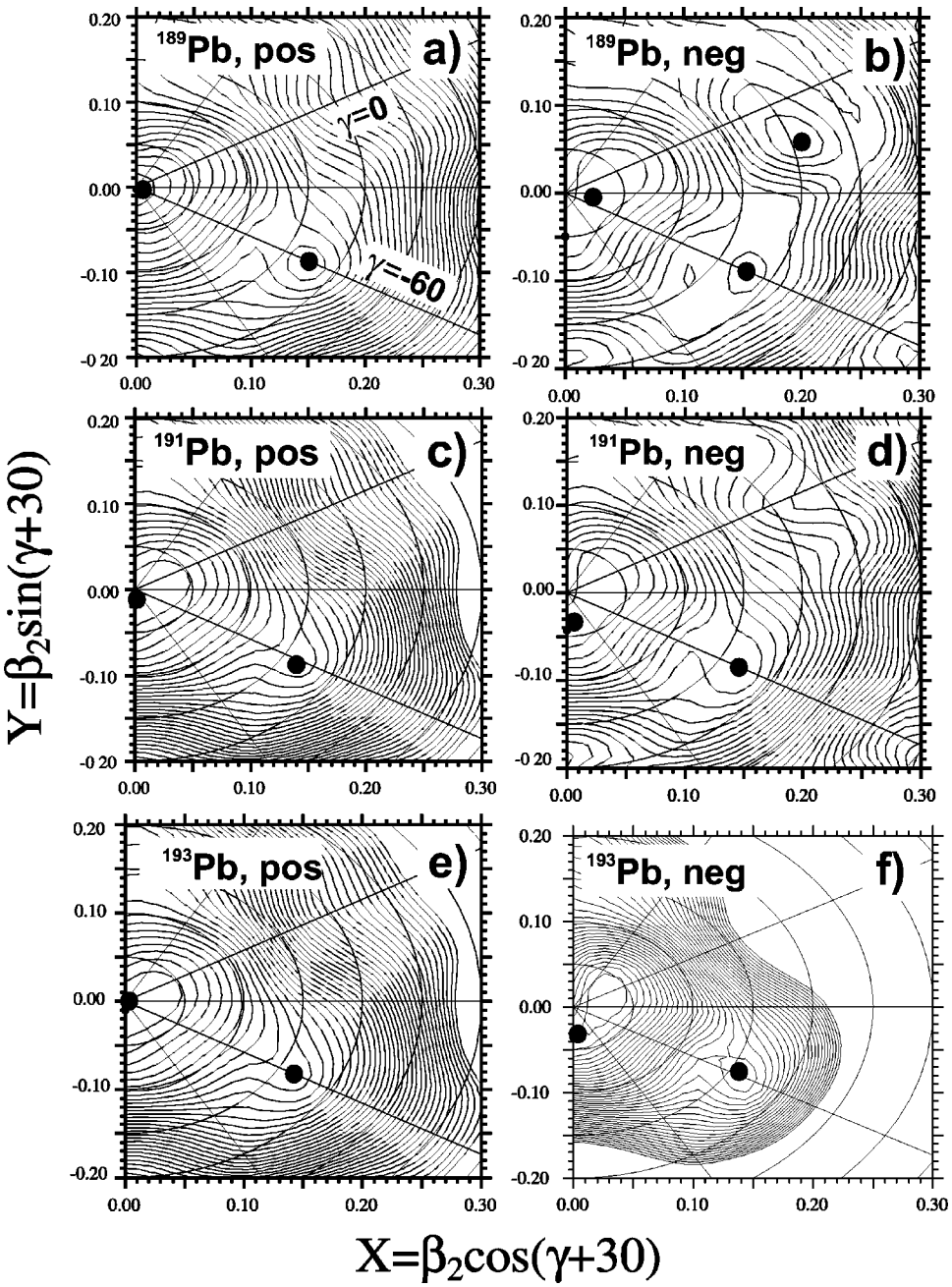

FIG. 5. Total potential energy surfaces for positive- and negative-parity states in ^{189}Pb (a),(b), ^{191}Pb (c),(d), and ^{193}Pb (e),(f). Positions of the spherical, oblate, and prolate minima are shown by dots. The contour lines are separated by 100 keV.

C. Potential energy surface calculations for the odd-mass lead nuclei

To further justify the intruder interpretation for the observed states, we performed PES calculations, details of the calculations can be found in Ref. [40]. These calculations were used to describe the odd-mass Po nuclei [28], while in the present work a summary of the results for the odd-mass lead nuclei is given. To check the reliability of the results, we performed PES calculations for the neighboring even-mass lead nuclei which provide extensive systematics for the intruder oblate 0^+ band heads; see Fig. 3. Rather good qualitative agreement between the calculated and experimental excitation energies of the deformed 0^+ bandheads relative to the spherical minimum was obtained, but quantitatively the calculated energy values are systematically about 500 keV higher than the experimental ones. One should mention that in Ref. [3] by using the same approach a rather good agreement between calculated and experimental excitation energies of the 0^+ oblate bandheads in the even-mass $^{196-202}$Po was obtained. All this gives us confidence with the results of the PES calculations. Potential energy surfaces for the positive and negative parity states in $^{189-193}$Pb are shown in Figs. 5(a)–5(f). In agreement with the experimental data, the dominant minimum in the PES of the positive- and negative-parity states in $^{189-199}$Pb corresponds to the occupation of the $1i_{13/2}$ or $3p_{3/2}$ neutron orbitals, respectively, producing spherical ($\beta_2 \leqslant 0.05$) $13/2^+$ or $3/2^-$ states lowest in energy. In addition, an excited oblate configuration ($\beta_2 \approx 0.18$, $\gamma \approx -60$) is predicted to coexist at low excitation energy, both for positive- and negative-parity states. In ^{193m,g}Pb these

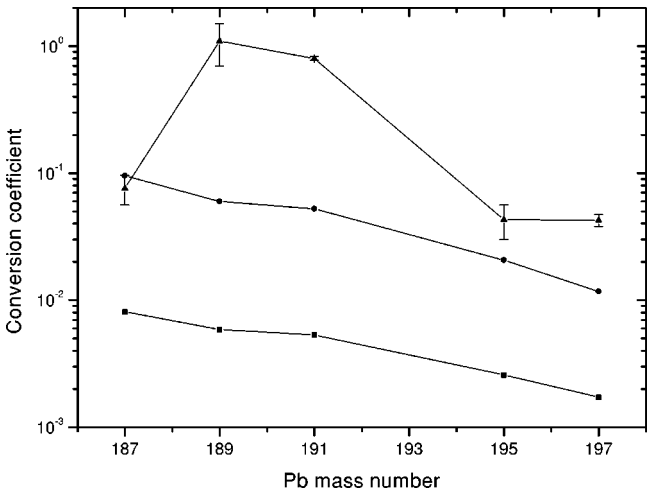

FIG. 6. Experimental (triangles) and theoretical $E2$ (squares) and $M1$ (circles) conversion coefficients for the transitions between the $13/2^+$ states in the odd-mass Pb nuclei. Experimental data for ^{187}Pb, ^{195}Pb, and ^{197}Pb are taken from [27,25,26], respectively. All values are total conversion coefficients, except for ^{187}Pb where K conversion coefficients are given.

minima are seen as shallow shoulders in the PES, which develop further and reach a minimum in excitation energy for ^{187m,g}Pb [28], while for lighter nuclei the oblate minimum is predicted to rise in energy and finally to disappear. Similar to the even-mass lead nuclei, the calculated energy values for the oblate states are higher compared to the experimental values (by $\approx$300 keV for the positive-parity states and by $\approx$200 keV for the negative-parity states). Nevertheless, the qualitative agreement between the measured and calculated energies—i.e., the trend of the excitation energy of these states as a function of neutron number in $^{189-193}$Pb—is rather good. A prolate minimum is predicted to lie $\approx$300 keV higher in energy than the oblate minimum in ^{189}Pb, while in the heavier odd-mass Pb nuclei the prolate minimum practically disappears. Thus, the results of the PES calculations strongly support the interpretation of the excited $13/2^+$ states in $^{189m-197m}$Pb and $3/2^-$ states in ^{189g,191g}Pb as oblate intruder states with $1i_{13/2}\otimes\pi(2p\text{-}2h)$ and $3p_{3/2}\otimes\pi(2p\text{-}2h)$ configurations, respectively.

D. $E0$ strength and mixing between coexisting shapes

Both fine-structure α-decay studies and PES calculations show a decrease in excitation energy of the deformed intruder states in the Pb isotopes when approaching the neutron midshell; in all cases the spherical state remains lowest in energy, but increased mixing between the low-lying coexisting shapes is expected. A direct measure of the mixing of the deformed intruder state and the spherical ground state is the $E0$ transition strength [41,42].

Lifetime measurements of the excited 0^+ intruder states in the even-mass ^{190,192,194}Pb isotopes indicate that the mixing between the deformed intruder state and the spherical state increases with decreasing neutron number [43], but in all cases the ground state is of mainly spherical character (up to 98% of the spherical component in the ground state of ^{190}Pb).

No exact values of mixing parameters through lifetime measurements could be deduced from the current experiment, but the conversion coefficients of the decay of the intruder states reveal some information about the mixing between the coexisting states. In Fig. 6 the experimental conversion coefficients for the transition between the $13/2^+$ states in odd-mass Pb isotopes are shown as a function of mass number. All values are total conversion coefficients, except for ^{187}Pb where K conversion coefficients are given. The data for ^{187}Pb, ^{195}Pb, and ^{197}Pb are taken from [28,25,26], respectively. In ^{195,197}Pb, $E0$ components have been observed in a number of transitions [25,26]. In this work, as we are only sensitive to the lowest-lying states, we will only discuss the transition from the first excited $13/2^+$ states. As mentioned before, the prompt decay of the intruder states limits the multipolarity to $\Delta L \leqslant 2$; the low hindrance factors of the α decay exclude a parity-changing transition. The experimental values therefore need to be compared with the theoretical values for $E2$ and $M1$ transitions only, in order to extract the contribution of the $E0$ component. Figure 6 shows small $E0$ components for the transition between the $13/2^+$ states in ^{195,197}Pb, indicating small mixing between the $13/2^+_2$ intruder state and the nearly spherical $13/2^+_1$ state. By moving to lower masses, in ^{191,189}Pb the $13/2^+$ intruder states drops down in energy and consequently the mixing of the oblate and nearly spherical $13/2^+$ states increases with a stronger $E0$ component as a consequence. However in ^{187}Pb this trend is interrupted and the experimental conversion coefficient can largely be explained by an $M1$ transition. Mixing due to possible coexistence of the oblate state with prolate states could be the cause for the reduction of the $E0$ strength in the transition connecting the oblate and near-spherical $13/2^+$ states [27,28]. In order to quantify the amount of mixing it is clear that dedicated experiments should be set up to derive the $E0$-$M1$-$E2$ strength.

V. CONCLUSIONS

In an α-decay study of ^{193,195,197}Po, produced in heavy-ion comlete fusion reactions and separated with the RITU gas-filled separator, fine structure in the α decay has been observed. The data provide information on the $\nu(1i_{13/2})\otimes\pi(2p\text{-}2h)$ intruder states in the $^{189m-193m}$Pb nuclei, extending the systematics of the $13/2^+$ oblate intruder states in the odd-mass lead nuclei from ^{197m}Pb down to the midshell nucleus ^{187}Pb. Oblate deformed $3/2^-$ intruder $\nu(3p_{3/2})\otimes\pi(2p\text{-}2h)$ states have been observed in ^{189g,191g}Pb as well. These intruder states deexcite to the nearly spherical states by transitions with different degree of conversion; qualitatively, the amount of $E0$ strength can be understood as due to mixing between the involved configurations. Together with theoretical potential energy surface calculations and in-beam and β-decay studies, the presented α-decay studies underline the richness of the neutron-deficient Pb region with its wealth of different shapes induced by only a small number of active nucleons.

ACKNOWLEDGMENTS

This work was supported by the Academy of Finland under the Finnish Center of Excellence Program 2000–2005 (Project No. 44875, Nuclear and Condensed Matter Physics Program at JYFL), the Access to Large Scale Facility program under the Training and Mobility of Researchers program of the European Union, by the FWO-Vlaanderen, and by the IUAP program, Belgium. K.V.d.V. is supported by FWO-Vlaanderen.

[1] K. Heyde *et al.*, Phys. Rep. **102**, 291 (1983).
[2] J.L. Wood *et al.*, Phys. Rep. **215**, 101 (1992).
[3] A. Oros *et al.*, Nucl. Phys. **A645**, 107 (1999).
[4] R. Julin *et al.*, J. Phys. G **27**, R109 (2001).
[5] F.R. May *et al.*, Phys. Lett. **68B**, 113 (1977).
[6] W. Nazarewicz, Phys. Lett. B **305**, 195 (1993).
[7] A.M. Baxter *et al.*, Phys. Rev. C **48**, 2140 (1993).
[8] J. Heese *et al.*, Phys. Lett. B **302**, 390 (1993).
[9] J.F.C. Cocks *et al.*, Eur. Phys. J. A **3**, 17 (1998).
[10] G.D. Dracoulis *et al.*, Phys. Lett. B **432**, 37 (1998).
[11] G.D. Dracoulis *et al.*, Phys. Rev. C **60**, 014303 (1999).
[12] N. Bijnens *et al.*, Phys. Rev. Lett. **75**, 4571 (1995).
[13] N. Bijnens *et al.*, Z. Phys. A **356**, 3 (1996).
[14] R.G. Allatt *et al.*, Phys. Lett. B **437**, 29 (1998).
[15] A.N. Andreyev *et al.*, J. Phys. G **25**, 835 (1999).
[16] Y. Le Coz *et al.*, EPJdirect **A3**, 1 (1999), http://link.springer.de/link/service/journals/10105/index.htm
[17] A.N. Andreyev *et al.*, Nature (London) **405**, 430 (2000).
[18] A.N. Andreyev *et al.*, Eur. Phys. J. A **6**, 381 (1999).
[19] D.G. Jenkins *et al.*, Phys. Rev. C **62**, 021302(R) (2000).
[20] P. Van Duppen *et al.*, Phys. Rev. Lett. **52**, 1974 (1984).
[21] R.B. Firestone, *Table of Isotopes* (Wiley, New York, 1996).
[22] A. Baxter *et al.*, Phys. Rev. C **58**, 2671 (1998).
[23] A. Baxter *et al.*, Department of Nuclear Physics, Australian National University, annual report, 1997 (unpublished), p. 33.
[24] N. Fotiades *et al.*, Phys. Rev. C **57**, 1624 (1998).
[25] J.G. Griffin *et al.*, Nucl. Phys. **A530**, 401 (1991).
[26] J. Vanhorenbeeck *et al.*, Nucl. Phys. **A531**, 63 (1991).
[27] A.N. Andreyev *et al.*, Phys. Rev. Lett. **82**, 1819 (1999).
[28] A.N. Andreyev *et al.*, Phys. Rev. C (submitted).
[29] A.N. Andreyev *et al.*, *Experimental Nuclear Physics in Europe*, edited by B. Rubia, M. Lezano, and W. Gelletly, AIP Conf. Proc. No. 495 (AIP, Melville, NY, 2000), p. 121.
[30] M. Leino *et al.*, Nucl. Instrum. Methods Phys. Res. B **99**, 653 (1995).
[31] J. Wauters *et al.*, Phys. Rev. C **47**, 1447 (1993).
[32] J. Wauters *et al.*, Phys. Rev. Lett. **72**, 1329 (1994).
[33] Computer code GEANT, Detector Simulation Tool, CERN, Geneva, 1993, http://wwwinfo.cern.ch/pl/GEANT and http://npg.de.ac.uk/GREAT/geant-gr.htm
[34] The National Nuclear Data Center (NNDC), http://www.nndc.bnl.gov/nndc/physco/
[35] Nucl. Data Sheets **15(2)**, 6 (1975).
[36] N. Fotiades *et al.*, Phys. Rev. C **56**, 723 (1997).
[37] J.O. Rasmussen, Phys. Rev. **113**, 1593 (1959).
[38] P. Van Duppen *et al.*, J. Phys. G **16**, 441 (1990).
[39] H. Kettunen *et al.*, Phys. Rev. C **63**, 044315 (2001).
[40] W. Satula and R. Wyss, Phys. Scr. **T56**, 159 (1995).
[41] K. Heyde and R.A. Meyer, Phys. Rev. C **37**, 2170 (1988).
[42] J.L. Wood *et al.*, Nucl. Phys. **A651**, 323 (1999).
[43] P. Dendooven *et al.*, Phys. Lett. B **226**, 27 (1989).